Efficient Implementation of Capon and APES for Spectral Estimation

ZHENG-SHE LIU

HONGBIN LI, Student Member, IEEE

JIAN LI, Senior Member, IEEE
University of Florida

Both the Capon and APES estimators can be shown to belong to the class of matched-filterbank spectral estimators and can be used to obtain complex spectral estimates that have more narrow spectral peaks and lower sidelobe levels than the fast Fourier transform (FFT) methods. It can also be shown that APES has better statistical performance than Capon. In this paper, we address the issue of how to efficiently implement Capon and APES for spectral estimation.

Manuscript received August 10, 1997; revised December 18, 1997.

IEEE Log No. T-AES/34/4/07984.

This work was supported in part by the Office of Naval Research Grant N00014-96-0817, the National Science Foundation Grant MIP-9457388, and the Advanced Research Project Agency Grant MDA-972-93-1-0015.

Authors' address: Dept. of Electrical and Computer Engineering, P.O. Box 116130, University of Florida, Gainesville, FL 32611.

I. INTRODUCTION

Complex spectral estimation is important in a variety of applications including target range signature estimation and synthetic aperture radar (SAR) imaging. Both the Capon [1] and APES [2] methods are adaptive finite impulse response (FIR) filtering based approaches that can be used to obtain complex spectral estimates with more narrow spectral peaks and lower sidelobes than the conventional fast Fourier transform (FFT) methods [2].

It has been shown in [3] that both Capon and APES belong to the class of matched-filterbank spectral estimators. However, Capon is proven to be biased downward whereas APES is unbiased (to within a second-order approximation) [3]. The theoretical results therein supplemented with the empirical observation that Capon usually underestimates the spectrum in samples of practical length while APES is nearly unbiased are believed to provide a compelling reason for preferring APES over Capon. However, the problem of how to efficiently implement Capon and APES has not been addressed carefully and the intuitive ways of implementing Capon and APES are computationally very expensive, especially for two-dimensional (2-D) spectral estimation from 2-D data sequences.

Here, we study how to implement Capon and APES efficiently. We only consider 2-D spectral estimation since one-dimensional spectral estimation is just a special case of what we consider herein. We show that the amount of computation required by APES is about 1.5 times that required by Capon. Furthermore, the efficient implementations of Capon and APES can significantly reduce the amount of computation needed by their intuitive implementations.

II. PROBLEM FORMULATION

Let $\{z_{n,\bar{n}},\ n = 0,1,\ldots,N-1,\ \bar{n} = 0,1,\ldots,\bar{N}-1\}$ denote a 2-D discrete-time data sequence. For a frequency pair $(\omega,\bar{\omega})$ of interest, we model $z_{n,\bar{n}}$ as

$$z_{n,\bar{n}} = \alpha(\omega,\bar{\omega})e^{j(n\omega+\bar{n}\bar{\omega})} + w_{n,\bar{n}}(\omega,\bar{\omega}),$$
$$n = 0,1,\ldots,N-1, \quad \bar{n} = 0,1,\ldots,\bar{N}-1 \qquad (1)$$

where $\alpha(\omega,\bar{\omega})$ denotes the complex amplitude of a 2-D sinusoid with frequency $(\omega,\bar{\omega})$ and $w_{n,\bar{n}}(\omega,\bar{\omega})$ denotes the unmodeled noise and interference at frequency $(\omega,\bar{\omega})$. The problem of interest is to obtain the estimate of $\alpha(\omega,\bar{\omega})$ from the 2-D data sequence for all $(\omega,\bar{\omega})$ of interest. In 2-D SAR imaging applications, for example, $\alpha(\omega,\bar{\omega})$ would be proportional to the radar cross section of a target scatterer located at a range proportional to ω and cross-range proportional to $\bar{\omega}$.

We describe below the efficient implementation of APES in detail since the discussion can be easily extended to the efficient implementation of Capon.

III. APES ESTIMATOR

Let $\mathbf{H}(\omega,\overline{\omega}) \in \mathcal{C}^{M\times\overline{M}}$ denote the impulse response of an $(M \times \overline{M})$-tap 2-D FIR filter and $\mathbf{Z}_{l,\bar{l}} = \{z_{n,\bar{n}},\ n = l,\ldots,l+M-1,\ \bar{n} = \bar{l},\ldots,\bar{l}+\overline{M}-1\},\ l = 0,\ldots,L-1,\ \bar{l} = 0,\ldots,\overline{L}-1$, be the overlapping matrix of the 2-D data sequence, where $L = N - M + 1$ and $\overline{L} = \overline{N} - \overline{M} + 1$. Let $\mathbf{h}(\omega,\overline{\omega}) = \text{vec}\{\mathbf{H}(\omega,\overline{\omega})\}$ and $\mathbf{z}_{l,\bar{l}} = \text{vec}\{\mathbf{Z}_{l,\bar{l}}\}$, where $\text{vec}\{\cdot\}$ denotes the operation consisting of stacking the columns of a matrix on top of each other. We have

$$\mathbf{h}^{\mathrm{H}}(\omega,\overline{\omega})\mathbf{z}_{l,\bar{l}} = \alpha(\omega,\overline{\omega})[\mathbf{h}^{\mathrm{H}}(\omega,\overline{\omega})\mathbf{a}_{M,\overline{M}}(\omega,\overline{\omega})] \times e^{j(l\omega+\bar{l}\overline{\omega})} + \xi_{l,\bar{l}}(\omega,\overline{\omega}) \tag{2}$$

where $(\cdot)^{\mathrm{H}}$ denotes complex conjugate transpose and $\mathbf{a}_{M,\overline{M}}(\omega,\overline{\omega}) = \mathbf{a}_{\overline{M}}(\overline{\omega}) \otimes \mathbf{a}_{M}(\omega)$, with $\mathbf{a}_M(\omega) = [1\ e^{j\omega}\ \cdots\ e^{j(M-1)\omega}]^{\mathrm{T}}$, $\otimes$ denoting the Kronecker product [4], and $\xi_{l,\bar{l}}(\omega,\overline{\omega}) = \mathbf{h}^{\mathrm{H}}(\omega,\overline{\omega})\mathbf{w}_{l,\bar{l}}(\omega,\overline{\omega})$ with $\mathbf{w}_{l,\bar{l}}(\omega,\overline{\omega})$ formed from $\{w_{n,\bar{n}}(\omega,\overline{\omega})\}$ in the same way as $\mathbf{z}_{l,\bar{l}}$ is formed from $\{z_{n,\bar{n}}\}$. Let $\mathbf{h}^{\mathrm{H}}(\omega,\overline{\omega})\mathbf{a}_{M,\overline{M}}(\omega,\overline{\omega}) = 1$. Then the least squares estimate of $\alpha(\omega,\overline{\omega})$ is

$$\hat{\alpha}(\omega,\overline{\omega}) = \frac{1}{\overline{L}L}\mathbf{h}^{\mathrm{H}}(\omega,\overline{\omega})\left[\sum_{\bar{l}=0}^{\overline{L}-1}\sum_{l=0}^{L-1}\mathbf{z}_{l,\bar{l}}e^{-j(l\omega+\bar{l}\overline{\omega})}\right]. \tag{3}$$

It has been shown in [2] that the (forward-and-backward) APES filter has the form

$$\mathbf{h}(\omega,\overline{\omega}) = \frac{\hat{\mathbf{Q}}^{-1}(\omega,\overline{\omega})\mathbf{a}_{M,\overline{M}}(\omega,\overline{\omega})}{\mathbf{a}^{\mathrm{H}}_{M,\overline{M}}(\omega,\overline{\omega})\hat{\mathbf{Q}}^{-1}(\omega,\overline{\omega})\mathbf{a}_{M,\overline{M}}(\omega,\overline{\omega})} \tag{4}$$

with

$$\hat{\mathbf{Q}}(\omega,\overline{\omega}) = \hat{\mathbf{R}} - [\mathbf{g}(\omega,\overline{\omega})\mathbf{g}^{\mathrm{H}}(\omega,\overline{\omega}) + \tilde{\mathbf{g}}(\omega,\overline{\omega})\tilde{\mathbf{g}}^{\mathrm{H}}(\omega,\overline{\omega})]/(\overline{L}L) \tag{5}$$

where

$$\hat{\mathbf{R}} = \hat{\overline{\mathbf{R}}} + \mathbf{J}\hat{\overline{\mathbf{R}}}^{\mathrm{T}}\mathbf{J} \tag{6}$$

$$\hat{\overline{\mathbf{R}}} = \sum_{\bar{l}=0}^{\overline{L}-1}\sum_{l=0}^{L-1}\mathbf{z}_{l,\bar{l}}\mathbf{z}^{\mathrm{H}}_{l,\bar{l}} \tag{7}$$

$$\mathbf{g}(\omega,\overline{\omega}) = \sum_{\bar{l}=0}^{\overline{L}-1}\sum_{l=0}^{L-1}\mathbf{z}_{l,\bar{l}}e^{-j(l\omega+\bar{l}\overline{\omega})} \tag{8}$$

$$\tilde{\mathbf{g}}(\omega,\overline{\omega}) = \sum_{\bar{l}=0}^{\overline{L}-1}\sum_{l=0}^{L-1}\tilde{\mathbf{z}}_{l,\bar{l}}e^{-j(l\omega+\bar{l}\overline{\omega})} \tag{9}$$

and where $\mathbf{J}$ denotes the exchange matrix (with ones on the cross-diagonal and zero elsewhere) with appropriate dimensions, and $\tilde{\mathbf{z}}_{l,\bar{l}} = \mathbf{J}\mathbf{z}^{*}_{L-l-1,\overline{L}-\bar{l}-1}$, with $(\cdot)^{*}$ denoting complex conjugate. By substituting (4) into (3), we obtain the APES estimate of $\alpha(\omega,\overline{\omega})$:

$$\hat{\alpha}_{\mathrm{APES}}(\omega,\overline{\omega}) = \frac{\mathbf{a}^{\mathrm{H}}_{M,\overline{M}}(\omega,\overline{\omega})\hat{\mathbf{Q}}^{-1}(\omega,\overline{\omega})\mathbf{g}(\omega,\overline{\omega})}{\overline{L}L\mathbf{a}^{\mathrm{H}}_{M,\overline{M}}(\omega,\overline{\omega})\hat{\mathbf{Q}}^{-1}(\omega,\overline{\omega})\mathbf{a}_{M,\overline{M}}(\omega,\overline{\omega})}. \tag{10}$$

IV. EFFICIENT IMPLEMENTATION OF APES

Let

$$\mathbf{Z} = [\mathbf{z}_{0,0}\ \cdots\ \mathbf{z}_{L-1,0}\ \cdots\ \mathbf{z}_{0,\overline{L}-1}\ \cdots\ \mathbf{z}_{L-1,\overline{L}-1}] \tag{11}$$

and $\tilde{\mathbf{Z}} = \mathbf{J}\mathbf{Z}^{*}\mathbf{J}$. We can then rewrite (8) and (9) as

$$\mathbf{g}(\omega,\overline{\omega}) = \mathbf{Z}\mathbf{a}^{*}_{L,\overline{L}}(\omega,\overline{\omega}) \tag{12}$$

and

$$\tilde{\mathbf{g}}(\omega,\overline{\omega}) = \tilde{\mathbf{Z}}\mathbf{a}^{*}_{L,\overline{L}}(\omega,\overline{\omega}). \tag{13}$$

By applying the matrix inversion lemma, we obtain

$$\hat{\mathbf{Q}}^{-1}(\omega,\overline{\omega}) = \tilde{\mathbf{Q}}^{-1}(\omega,\overline{\omega}) + \frac{\tilde{\mathbf{Q}}^{-1}(\omega,\overline{\omega})\mathbf{g}(\omega,\overline{\omega})\mathbf{g}^{\mathrm{H}}(\omega,\overline{\omega})\tilde{\mathbf{Q}}^{-1}(\omega,\overline{\omega})}{\overline{L}L - \mathbf{g}^{\mathrm{H}}(\omega,\overline{\omega})\tilde{\mathbf{Q}}^{-1}(\omega,\overline{\omega})\mathbf{g}(\omega,\overline{\omega})} \tag{14}$$

where

$$\tilde{\mathbf{Q}}^{-1}(\omega,\overline{\omega}) = \hat{\mathbf{R}}^{-1} + \frac{\hat{\mathbf{R}}^{-1}\tilde{\mathbf{g}}(\omega,\overline{\omega})\tilde{\mathbf{g}}^{\mathrm{H}}(\omega,\overline{\omega})\hat{\mathbf{R}}^{-1}}{\overline{L}L - \tilde{\mathbf{g}}^{\mathrm{H}}(\omega,\overline{\omega})\hat{\mathbf{R}}^{-1}\tilde{\mathbf{g}}(\omega,\overline{\omega})}. \tag{15}$$

(For notational convenience, we sometimes drop the dependence on ω and $\overline{\omega}$ below.) Hence,

$$\begin{aligned}\mathbf{a}^{\mathrm{H}}_{M,\overline{M}}(\omega,\overline{\omega})\hat{\mathbf{Q}}^{-1}(\omega,\overline{\omega})\mathbf{g}(\omega,\overline{\omega}) &= \mathbf{a}^{\mathrm{H}}_{M,\overline{M}}\tilde{\mathbf{Q}}^{-1}\mathbf{g} + \frac{\mathbf{a}^{\mathrm{H}}_{M,\overline{M}}\tilde{\mathbf{Q}}^{-1}\mathbf{g}\mathbf{g}^{\mathrm{H}}\tilde{\mathbf{Q}}^{-1}\mathbf{g}}{\overline{L}L - \mathbf{g}^{\mathrm{H}}\tilde{\mathbf{Q}}^{-1}\mathbf{g}} \\ &= \frac{\overline{L}L\mathbf{a}^{\mathrm{H}}_{M,\overline{M}}\tilde{\mathbf{Q}}^{-1}\mathbf{g}}{\overline{L}L - \mathbf{g}^{\mathrm{H}}\tilde{\mathbf{Q}}^{-1}\mathbf{g}}\end{aligned} \tag{16}$$

and

$$\begin{aligned}\mathbf{a}^{\mathrm{H}}_{M,\overline{M}}(\omega,\overline{\omega})\hat{\mathbf{Q}}^{-1}\mathbf{a}_{M,\overline{M}}(\omega,\overline{\omega}) &= \mathbf{a}^{\mathrm{H}}_{M,\overline{M}}\tilde{\mathbf{Q}}^{-1}\mathbf{a}_{M,\overline{M}} + \frac{|\mathbf{a}^{\mathrm{H}}_{M,\overline{M}}\tilde{\mathbf{Q}}^{-1}\mathbf{g}|^2}{\overline{L}L - \mathbf{g}^{\mathrm{H}}\tilde{\mathbf{Q}}^{-1}\mathbf{g}}.\end{aligned} \tag{17}$$

It follows that (10) can be rewritten as

$$\hat{\alpha}_{\mathrm{APES}}(\omega,\overline{\omega}) = \frac{\mathbf{a}^{\mathrm{H}}_{M,\overline{M}}\tilde{\mathbf{Q}}^{-1}\mathbf{g}}{(\overline{L}L - \mathbf{g}^{\mathrm{H}}\tilde{\mathbf{Q}}^{-1}\mathbf{g})\mathbf{a}^{\mathrm{H}}_{M,\overline{M}}\tilde{\mathbf{Q}}^{-1}\mathbf{a}_{M,\overline{M}} + |\mathbf{a}^{\mathrm{H}}_{M,\overline{M}}\tilde{\mathbf{Q}}^{-1}\mathbf{g}|^2}. \tag{18}$$

Since $\hat{\mathbf{R}}$ is Hermitian and positive definite, we can obtain an upper triangular matrix $\hat{\mathbf{C}}$ by Cholesky factorization such that $\hat{\mathbf{R}}^{-1} = \hat{\mathbf{C}}^{-1}(\hat{\mathbf{C}}^{-1})^{\mathrm{H}}$ [5]. Let

$$\mathbf{b}^T(\omega,\overline{\omega}) = \mathbf{a}^{\mathrm{H}}_{M,\overline{M}}(\omega,\overline{\omega})\hat{\mathbf{C}}^{-1} \tag{19}$$

$$\mathbf{d}(\omega,\overline{\omega}) = \mathbf{D}\mathbf{a}^{*}_{L,\overline{L}}(\omega,\overline{\omega}) \tag{20}$$

and

$$\mathbf{e}(\omega,\overline{\omega}) = \mathbf{E}\mathbf{a}^{*}_{L,\overline{L}}(\omega,\overline{\omega}) \tag{21}$$

where $\mathbf{D} = (\hat{\mathbf{C}}^{-1})^{\mathrm{H}}\mathbf{Z}$ and $\mathbf{E} = (\hat{\mathbf{C}}^{-1})^{\mathrm{H}}\tilde{\mathbf{Z}}$. We have

$$\begin{aligned}\mathbf{a}^{\mathrm{H}}_{M,\overline{M}}\tilde{\mathbf{Q}}^{-1}\mathbf{g} &= \mathbf{a}^{\mathrm{H}}_{M,\overline{M}}\hat{\mathbf{R}}^{-1}\mathbf{g} + \frac{\mathbf{a}^{\mathrm{H}}_{M,\overline{M}}\hat{\mathbf{R}}^{-1}\tilde{\mathbf{g}}\tilde{\mathbf{g}}^{\mathrm{H}}\hat{\mathbf{R}}^{-1}\mathbf{g}}{\overline{L}\overline{L} - \tilde{\mathbf{g}}^{\mathrm{H}}\hat{\mathbf{R}}^{-1}\tilde{\mathbf{g}}} \\ &= \mathbf{b}^T(\omega,\overline{\omega})\mathbf{d}(\omega,\overline{\omega}) \\ &\quad + \frac{\mathbf{b}^T(\omega,\overline{\omega})\mathbf{e}(\omega,\overline{\omega})\mathbf{e}^{\mathrm{H}}(\omega,\overline{\omega})\mathbf{d}(\omega,\overline{\omega})}{\overline{L}\overline{L} - \|\mathbf{e}(\omega,\overline{\omega})\|^2}\end{aligned} \tag{22}$$

$$\begin{aligned}\mathbf{g}^{\mathrm{H}}\tilde{\mathbf{Q}}^{-1}\mathbf{g} &= \mathbf{g}^{\mathrm{H}}\hat{\mathbf{R}}^{-1}\mathbf{g} + \frac{\mathbf{g}^{\mathrm{H}}\hat{\mathbf{R}}^{-1}\tilde{\mathbf{g}}\tilde{\mathbf{g}}^{\mathrm{H}}\hat{\mathbf{R}}^{-1}\mathbf{g}}{\overline{L}\overline{L} - \tilde{\mathbf{g}}^{\mathrm{H}}\hat{\mathbf{R}}^{-1}\tilde{\mathbf{g}}} \\ &= \|\mathbf{d}(\omega,\overline{\omega})\|^2 + \frac{|\mathbf{d}^{\mathrm{H}}(\omega,\overline{\omega})\mathbf{e}(\omega,\overline{\omega})|^2}{\overline{L}\overline{L} - \|\mathbf{e}(\omega,\overline{\omega})\|^2}\end{aligned} \tag{23}$$

and

$$\begin{aligned}\mathbf{a}^{\mathrm{H}}_{M,\overline{M}}\tilde{\mathbf{Q}}^{-1}\mathbf{a}_{M,\overline{M}} &= \mathbf{a}^{\mathrm{H}}_{M,\overline{M}}\hat{\mathbf{R}}^{-1}\mathbf{a}_{M,\overline{M}} + \frac{\mathbf{a}^{\mathrm{H}}_{M,\overline{M}}\hat{\mathbf{R}}^{-1}\tilde{\mathbf{g}}\tilde{\mathbf{g}}^{\mathrm{H}}\hat{\mathbf{R}}^{-1}\mathbf{a}_{M,\overline{M}}}{\overline{L}\overline{L} - \tilde{\mathbf{g}}^{\mathrm{H}}\hat{\mathbf{R}}^{-1}\tilde{\mathbf{g}}} \\ &= \|\mathbf{b}(\omega,\overline{\omega})\|^2 + \frac{|\mathbf{b}^T(\omega,\overline{\omega})\mathbf{e}(\omega,\overline{\omega})|^2}{\overline{L}\overline{L} - \|\mathbf{e}(\omega,\overline{\omega})\|^2}.\end{aligned} \tag{24}$$

Next we observe that $\mathbf{b}(\omega,\overline{\omega})$, $\mathbf{d}(\omega,\overline{\omega})$, and $\mathbf{e}(\omega,\overline{\omega})$ can be calculated via 2-D FFT. Specifically, we partition $\hat{\mathbf{C}}^{-1}$, $\mathbf{D}$, and $\mathbf{E}$ as follows: $\hat{\mathbf{C}}^{-1} = [\mathrm{vec}\{\mathbf{B}_1\} \cdots \mathrm{vec}\{\mathbf{B}_{M\overline{M}}\}]$, $\mathbf{D} = [\mathrm{vec}\{\mathbf{D}_1\} \cdots \mathrm{vec}\{\mathbf{D}_{M\overline{M}}\}]^{\mathrm{T}}$, and $\mathbf{E} = [\mathrm{vec}\{\mathbf{E}_1\} \cdots \mathrm{vec}\{\mathbf{E}_{M\overline{M}}\}]^{\mathrm{T}}$, where $\mathbf{B}_k \in \mathcal{C}^{M\times\overline{M}}$, $\mathbf{D}_k \in \mathcal{C}^{L\times\overline{L}}$ and $\mathbf{E}_k \in \mathcal{C}^{L\times\overline{L}}$. Then (again, we drop the dependence on ω and $\overline{\omega}$)

$$\begin{aligned}\mathbf{b}^{\mathrm{T}} &= \mathbf{a}^{\mathrm{H}}_{M,\overline{M}}\hat{\mathbf{C}}^{-1} \\ &= [(\mathbf{a}^{\mathrm{H}}_{\overline{M}} \otimes \mathbf{a}^{\mathrm{H}}_{M})\mathrm{vec}\{\mathbf{B}_1\} \quad \cdots \quad (\mathbf{a}^{\mathrm{H}}_{\overline{M}} \otimes \mathbf{a}^{\mathrm{H}}_{M})\mathrm{vec}\{\mathbf{B}_{M\overline{M}}\}] \\ &= [\mathbf{a}^{\mathrm{H}}_{M}\mathbf{B}_1\mathbf{a}^{*}_{\overline{M}} \quad \cdots \quad \mathbf{a}^{\mathrm{H}}_{M}\mathbf{B}_{M\overline{M}}\mathbf{a}^{*}_{\overline{M}}].\end{aligned} \tag{25}$$

Likewise, we have

$$\mathbf{d} = \mathbf{D}\mathbf{a}^{*}_{L,\overline{L}} = [\mathbf{a}^{\mathrm{H}}_{L}\mathbf{D}_1\mathbf{a}^{*}_{\overline{L}} \quad \cdots \quad \mathbf{a}^{\mathrm{H}}_{L}\mathbf{D}_{M\overline{M}}\mathbf{a}^{*}_{\overline{L}}]^{\mathrm{T}} \tag{26}$$

and

$$\mathbf{e} = \mathbf{E}\mathbf{a}^{*}_{L,\overline{L}} = [\mathbf{a}^{\mathrm{H}}_{L}\mathbf{E}_1\mathbf{a}^{*}_{\overline{L}} \quad \cdots \quad \mathbf{a}^{\mathrm{H}}_{L}\mathbf{E}_{M\overline{M}}\mathbf{a}^{*}_{\overline{L}}]^{\mathrm{T}}. \tag{27}$$

Note that $\mathbf{a}^{\mathrm{H}}_{M}\mathbf{B}_k\mathbf{a}^{*}_{\overline{M}}$ denotes the 2-D discrete Fourier transform of $\mathbf{B}_k$ at $(\omega,\overline{\omega})$. Hence APES can be efficiently implemented by first calculating $\mathbf{b}(\omega,\overline{\omega})$, $\mathbf{d}(\omega,\overline{\omega})$, and $\mathbf{e}(\omega,\overline{\omega})$ via 2-D FFT, then using (22), (23), and (24) to determine $\mathbf{a}^{\mathrm{H}}_{M,\overline{M}}\tilde{\mathbf{Q}}^{-1}\mathbf{g}$, $\mathbf{g}^{\mathrm{H}}\tilde{\mathbf{Q}}^{-1}\mathbf{g}$, and $\mathbf{a}^{\mathrm{H}}_{M,\overline{M}}\tilde{\mathbf{Q}}^{-1}\mathbf{a}_{M,\overline{M}}$, respectively, and finally using (18) to obtain $\hat{\alpha}_{\mathrm{APES}}(\omega,\overline{\omega})$.

Let $\boldsymbol{\mu}_1(\omega,\overline{\omega}) = \hat{\mathbf{R}}^{-1/2}\mathbf{a}_{M,\overline{M}}(\omega,\overline{\omega})$, $\boldsymbol{\mu}_2(\omega,\overline{\omega}) = \hat{\mathbf{R}}^{-1/2}\mathbf{g}_{M,\overline{M}}(\omega,\overline{\omega})/(L\overline{L})$, and $\boldsymbol{\mu}_3(\omega,\overline{\omega}) = \hat{\mathbf{R}}^{-1/2}\tilde{\mathbf{g}}_{M,\overline{M}}(\omega,\overline{\omega})/(L\overline{L})$, The intuitive implementation of APES suggested in [3] has the form:

$$\hat{\alpha}_{\mathrm{APES}}(\omega,\overline{\omega}) = \frac{\boldsymbol{\mu}_1^{\mathrm{H}}\boldsymbol{\mu}_2 - \frac{1}{2}[\boldsymbol{\mu}_1^{\mathrm{H}}\boldsymbol{\mu}_2 \quad \boldsymbol{\mu}_1^{\mathrm{H}}\boldsymbol{\mu}_3]\Xi^{-1}\begin{bmatrix}\|\boldsymbol{\mu}_2\|^2 \\ \boldsymbol{\mu}_3^{\mathrm{H}}\boldsymbol{\mu}_2\end{bmatrix}}{\|\boldsymbol{\mu}_1\|^2 - \frac{1}{2}[\boldsymbol{\mu}_1^{\mathrm{H}}\boldsymbol{\mu}_2 \quad \boldsymbol{\mu}_1^{\mathrm{H}}\boldsymbol{\mu}_3]\Xi^{-1}\begin{bmatrix}\boldsymbol{\mu}_2^{\mathrm{H}}\boldsymbol{\mu}_1 \\ \boldsymbol{\mu}_3^{\mathrm{H}}\boldsymbol{\mu}_1\end{bmatrix}} \tag{28}$$

where

$$\Xi = \frac{1}{2}\begin{bmatrix}\|\boldsymbol{\mu}_2\|^2 & \boldsymbol{\mu}_2^{\mathrm{H}}\boldsymbol{\mu}_3 \\ \boldsymbol{\mu}_3^{\mathrm{H}}\boldsymbol{\mu}_2 & \|\boldsymbol{\mu}_3\|^2\end{bmatrix} - \mathbf{I}$$

with $\mathbf{I}$ denoting the 2×2 identity matrix.

The structure of (28) is similar to that of (18). However, the amount of computation required by the former is much larger than that by the latter. The reason is that, even though $\mathbf{g}_{M,\overline{M}}(\omega,\overline{\omega})$ and $\tilde{\mathbf{g}}_{M,\overline{M}}(\omega,\overline{\omega})$ can be obtained by 2-D FFT, for each $(\omega,\overline{\omega})$ pair, we have to compute the additional matrix-vector products $\hat{\mathbf{R}}^{-1/2}\mathbf{g}_{M,\overline{M}}(\omega,\overline{\omega})$ and $\hat{\mathbf{R}}^{-1/2}\tilde{\mathbf{g}}_{M,\overline{M}}(\omega,\overline{\omega})$ (recall that $\hat{\mathbf{R}}^{-1/2} \in \mathcal{C}^{M\overline{M}\times M\overline{M}}$, $\mathbf{g}_{M,\overline{M}}(\omega,\overline{\omega})$ and $\mathbf{g}_{M,\overline{M}}(\omega,\overline{\omega}) \in \mathcal{C}^{M\overline{M}\times 1}$) to obtain $\boldsymbol{\mu}_2(\omega,\overline{\omega})$ and $\boldsymbol{\mu}_3(\omega,\overline{\omega})$. On the other hand, by computing $\mathbf{D}$ and $\mathbf{E}$ first (which are computed only once), we bypass calculating such matrix-vector products and save a large amount of computation. The larger the number of samples in the 2-D frequency domain, the more the amount of computation we save. These discussions also apply to the implementation of Capon.

V. EXTENSION TO CAPON

It has been shown in [2] that APES becomes Capon when $\hat{\mathbf{Q}}(\omega,\overline{\omega})$ is replaced by $\hat{\mathbf{R}}$. Hence the efficient implementation of Capon can readily be achieved by modifying (18) as follows:

$$\hat{\alpha}_{\mathrm{Capon}}(\omega,\overline{\omega}) = \frac{\mathbf{b}^{\mathrm{T}}(\omega,\overline{\omega})\mathbf{d}(\omega,\overline{\omega})}{L\overline{L}\|\mathbf{b}(\omega,\overline{\omega})\|^2}. \tag{29}$$

Hence the efficient implementation of Capon is by using (19) and (20) to calculate $\mathbf{b}(\omega,\overline{\omega})$ and $\mathbf{d}(\omega,\overline{\omega})$, respectively, and then using them in (29). Since the amount of computation required to calculate $\mathbf{b}(\omega,\overline{\omega})$ in (19), $\mathbf{d}(\omega,\overline{\omega})$ in (20), or $\mathbf{e}(\omega,\overline{\omega})$ in (21) is approximately the same and calculating $\hat{\alpha}_{\mathrm{APES}}(\omega,\overline{\omega})$ by (18) and $\hat{\alpha}_{\mathrm{Capon}}(\omega,\overline{\omega})$ by (29) are much less involved than obtaining $\mathbf{b}(\omega,\overline{\omega})$, $\mathbf{d}(\omega,\overline{\omega})$, and $\mathbf{e}(\omega,\overline{\omega})$, the total amount of computation required by APES is about

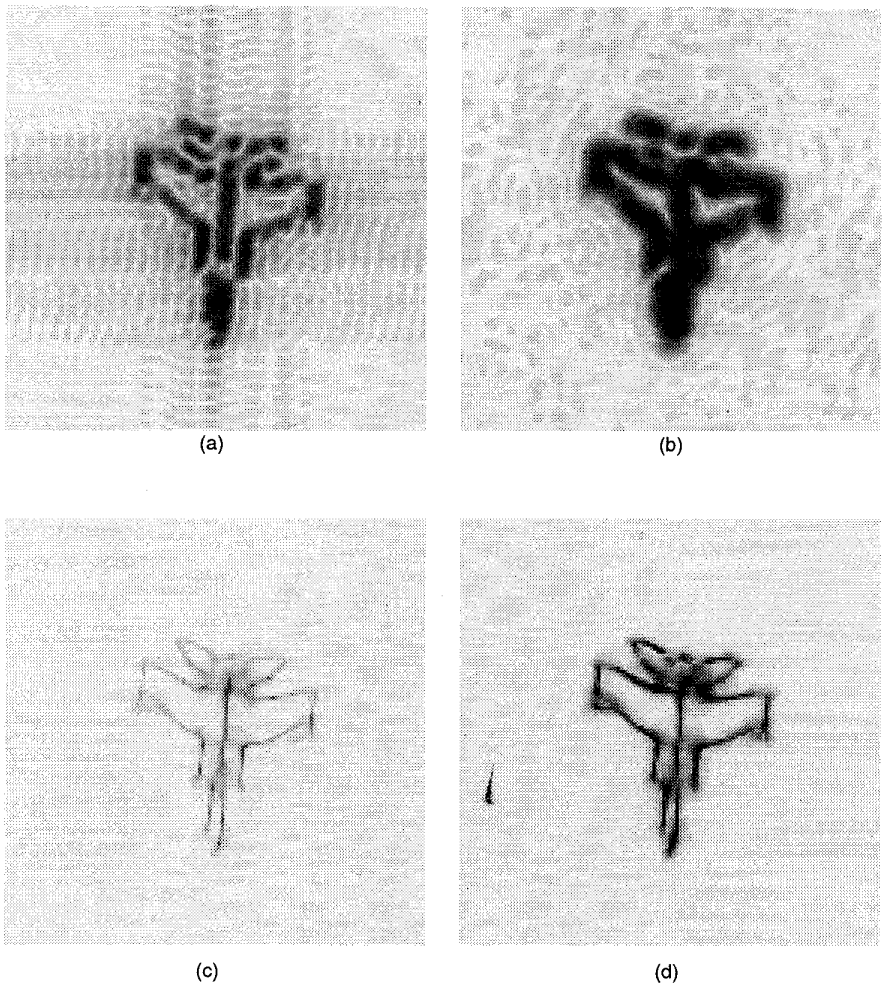

Fig. 1. SAR images of simulated MIG-25 airplane obtained by using (a) 2-D FFT, (b) 2-D windowed FFT, (c) 2-D Capon, (d) 2-D APES.

1.5 times that required by Capon, as verified by the numerical and experimental examples in Section VI.

The intuitive implementation of Capon has the form [3]:

$$\hat{\alpha}_{\text{Capon}}(\omega,\overline{\omega}) = \frac{\boldsymbol{\mu}_1^{\text{H}}(\omega,\overline{\omega})\boldsymbol{\mu}_2(\omega,\overline{\omega})}{\|\boldsymbol{\mu}_1(\omega,\overline{\omega})\|^2}. \tag{30}$$

Again, for similar reasons as for APES, this intuitive implementation of Capon is computationally more involved than the efficient implementation of Capon proposed above.

VI. NUMERICAL AND EXPERIMENTAL EXAMPLES

We present numerical and experimental examples comparing the performances of APES and Capon with the FFT methods [2] for SAR imaging. In the following examples, we choose $M = N/2$ and $\overline{M} = \overline{N}/2$ for both Capon and APES. (Note that choosing smaller values of M and $\overline{M}$ improves the accuracy of the Capon estimates at the cost of poorer resolution. See [2, 3] for details. We compare herein the computational complexity only when identical parameters are used.) For the windowed FFT method, we use the Kaiser window with parameter 4.

We first consider SAR imaging of a simulated MIG-25 airplane. The 32×32 data matrix was provided to us by the Naval Research Laboratory. The 128×128 SAR images obtained by using 2-D FFT, 2-D windowed FFT, 2-D Capon, and 2-D APES are shown in Figs. 1(a)–(d), respectively. We note that Capon and APES outperform the FFT methods. The number of flops required by our efficient ways of implementing Capon and APES are about 950 and 1500 times those required by the FFT methods, while those required by the intuitive ways of implementing Capon and APES are about 22800 and 30000 times, respectively, those required by the FFT methods. That is, the number of flops required by the intuitive ways of implementing Capon and APES are, respectively, about 24 and 20 times of those required by our efficient ways of implementing them. If we increase

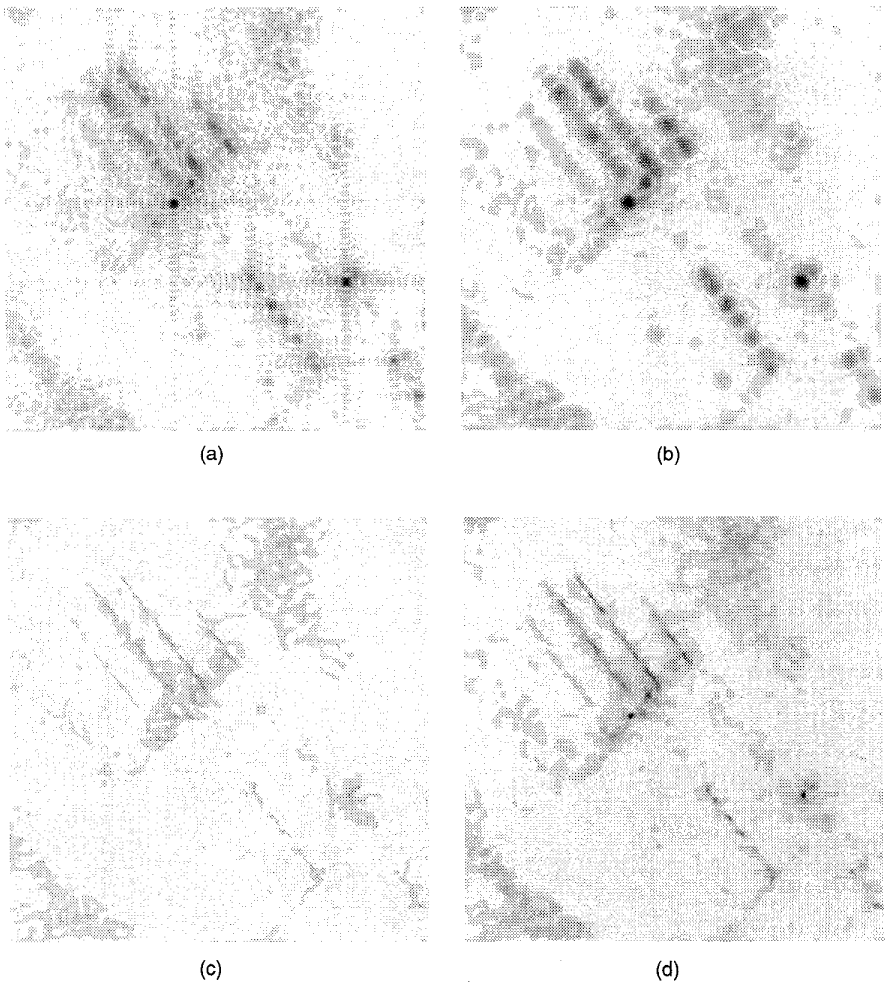

Fig. 2. SAR images obtained from ERIM data by using (a) 2-D FFT, (b) 2-D windowed FFT, (c) 2-D Capon, (d) 2-D APES.

the size of the image to 256×256 and 512×512, respectively, the ratios of the needed flops between the intuitive ways and our new ways for implementations are 36 and 40 for Capon, and 31 and 34 for APES, respectively.

We now consider an example of SAR imaging with experimental data. The data matrix is 64×64 and is obtained from the experimental data collected by one of the two apertures of the ERIM's (Environmental Research Institute of Michigan) DCS IFSAR (interferometric SAR). The 256×256 SAR image obtained by using 2-D FFT, 2-D windowed FFT, 2-D Capon, and 2-D APES are shown in Figs. 2(a)–(d), respectively. Again, Capon and APES outperform the FFT methods. The number of flops required by the intuitive ways of implementing Capon and APES are, respectively, about 38 and 32 times those required by our efficient ways of implementing them. If we increase the size of the image to 512×512, the ratios of the needed flops between the intuitive ways and our new ways of implementing Capon and APES are 86 and 73, respectively.

VII. CONCLUSIONS

We have presented computationally efficient ways of implementing both Capon and APES. We have shown that the amount of computation required by APES is about 1.5 times that required by Capon. Furthermore, the amount of computation required by our proposed approach is significantly reduced as compared with those needed by the existing intuitive methods.

REFERENCES

[1] Capon, J. (1969)
High resolution frequency-wavenumber spectrum analysis.
Proceedings of IEEE, **57** (Aug. 1969), 1408–1418.

[2] Li, J., and Stoica, P. (1996)
An adaptive filtering approach to spectral estimation and SAR imaging.
IEEE Transactions on Signal Processing, **44** (June 1996), 1469–1484.

[3] Li, H., Li, J., and Stoica, P. (1998)
Performance analysis of forward-backward matched-filterbank spectral estimators.
IEEE Transactions on Signal Processing, **46** (July 1998), 1954–1966.

[4] Graham, A. (1981)
Kronecker Products and Matrix Calculus with Applications.
Chichester, UK: Ellis Horwood Ltd., 1981.

[5] Golub, G. H., and Van Loan, C. F. (1984)
Matrix Computations.
Baltimore, MD: The Johns Hopkins University Press, 1984.

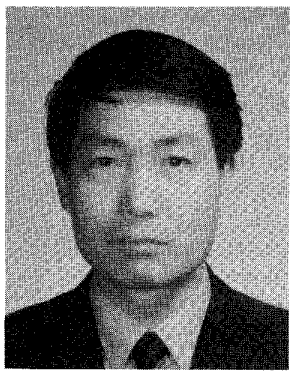

Zheng-She Liu received the M.Sc. and Ph.D. degrees in control engineering from Beijing University of Aeronautics and Astronautics, Beijing, China, in 1984 and 1990, respectively.

From December 1984 to January 1995, he was an Assistant Lecturer, Lecturer, and Associate Professor with the Department of Control Engineering, Beijing University of Aeronautics and Astronautics. From January 1995 to October 1997, he was a Visiting Scholar with the Department of Electrical and Computer Engineering, University of Florida, Gainesville. Since October 1997, he has been a Senior Engineer with the Personal Communication Division, US Robotics/3Com, Stokie, IL. His current research interests include digital signal processing, system simulation, and digital communications.

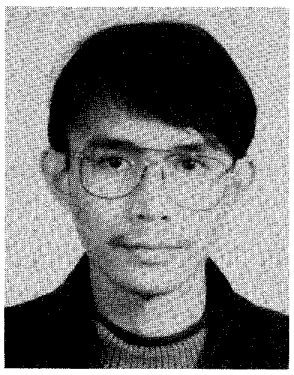

Hongbin Li (S'98) received the B.S. degree in 1991 and M.S. degree in 1994 from the University of Electronic Science and Technology of China (UESTC), Chengdu, China, all in electrical engineering. He is currently pursuing the Ph.D. degree in electrical engineering at the University of Florida, Gainesville, FL.

From April 1994 to December 1995, he was an Assistant Lecturer at the UESTC. Since 1996, he has been with the Spectral Analysis Laboratory at the University of Florida as a Research Assistant. His current research interests include digital signal processing, detection and estimation, and communications.

Mr. Li is a member of Tau Beta Pi.

Jian Li (S'87—M'91—SM'97) received the M.Sc. and Ph.D. degrees in electrical engineering from The Ohio State University, Columbus, in 1987 and 1991, respectively.

From April 1991 to June 1991, she was an Adjunct Assistant Professor with the Department of Electrical Engineering, The Ohio State University, Columbus. From July 1991 to June 1993, she was an Assistant Professor with the Department of Electrical Engineering, University of Kentucky, Lexington. Since August 1993, she has been with the Department of Electrical and Computer Engineering, University of Florida, Gainesville, where she is currently an Associate Professor. Her current research interests include spectral estimation, synthetic aperture radar image formation and understanding, radar detection and estimation theory, sensor array signal processing, image segmentation and processing, and communications.

Dr. Li is a member of Sigma Xi and Phi Kappa Phi. She received the 1994 National Science Foundation Young Investigator Award and the 1996 Office of Naval Research Young Investigator Award.